



Efforts for long-term protection of palladium hydrodechlorination catalysts

Daniele Comandella, Silke Woszidlo, Anett Georgi, Frank-Dieter Kopinke, Katrin Mackenzie*

Helmholtz Centre for Environmental Research—UFZ, Department of Environmental Engineering, D-04318 Leipzig, Germany

ARTICLE INFO

Article history:

Received 2 September 2015

Received in revised form

17 December 2015

Accepted 28 December 2015

Available online 2 January 2016

Keywords:

Pd hydrodechlorination catalysts

Catalyst coating

Catalyst deactivation

Catalyst long-term activity

Water treatment

ABSTRACT

Nano-sized palladium (Pd) catalysts are known for their high intrinsic hydrodechlorination (HDC) activity towards many chlorinated water pollutants, converting them into non-harmful compounds. Optimization of catalyst protection by embedding various types of Pd catalysts (Pd on oxitic supports and *in-situ* generated Pd clusters) into poly(dimethylsiloxane) (PDMS) layers was studied together with their use in HDC reactions. The catalyst performance in standard batch and long-term experimental set-ups was used to better understand and optimize the Pd-PDMS system. The phenomenon of polymer deterioration by entrapped HDC-generated HCl is studied for various systems and found to be the main reason for limited life times of Pd-PDMS systems.

Pd-PDMS composites were found to provide long-term protection from ionic catalyst poisons. This gain in prolonged catalyst protection goes along with an inevitable decrease in specific catalyst activity which is unhesitantly accepted for the benefit of a longer-lasting catalytic activity. However, when comparing the relative loss of the specific Pd activity due to embedding, it is found to be much lower for initially less active catalyst particles (e.g. a factor of 2 for Pd/Al₂O₃) compared to about two orders of magnitude for the highly active nanoscale Pd particles. It could be shown that embedded catalysts in continuously operated long-term set-ups have enhanced resistance and longevity compared to those tested in repeated batch-type reaction cycles. PDMS-embedded Pd/Al₂O₃ maintains its full initial activity up to turnover numbers of >750 (for trichloroethene as probe substance), whereas the catalyst system loses more than 50% of its initial activity for a comparable catalyst utilization (TON ≈ 750) operated in batch cycles.

© 2016 Elsevier B.V. All rights reserved.

1. Introduction

Traditional chlorinated hydrocarbons (CHCs) and emerging chlorinated contaminants are among the most widely distributed pollutants in water. Their dechlorination to environmentally harmless compounds is a significant contribution towards cleaner water resources. Together with hydrogen donors, such as molecular hydrogen (H₂), Pd catalysts are able to perform under ambient conditions fast hydrodechlorination (HDC) of a broad range of chlorinated contaminants, converting them to non-harmful products [1–4]. Compared with other transition-metal-based catalysts, such as Rh, Pt or Ni, Pd catalysts are characterized by higher selectivity, activity, stability and a lower toxicity, and are therefore particularly appropriate for a rapid and effective water treatment [4–6]. In the case of chlorinated ethenes, of which PCE and TCE are widely distributed groundwater pollutants, Pd catalyses the substitution of

chlorine by hydrogen atoms and the saturation of the double bond, forming ethane and hydrochloric acid. The high intrinsic specific activity of Pd A_{Pd} in terms of L of water per g of palladium per min (Lg⁻¹ min⁻¹), which is equivalent to a second-order rate coefficient k_i [7], becomes evident when using nanostructured catalysts [8–10]. For example, a specific Pd activity of 22,500 Lg⁻¹ min⁻¹ was reached for TCE hydrodechlorination using Pd on nanomagnetite (Pd/Fe₃O₄) in clean waters [8]. This was the highest activity ever recorded for a Pd catalyst in a HDC reaction. Nevertheless, the few tests under field conditions led to much lower specific Pd activities of about 0.1 Lg⁻¹ min⁻¹ in real groundwaters [11–13]. The dramatic loss in reaction rates compared with laboratory-scale experiments is caused not only by common external (bulk to surface) and internal (diffusion into pores) mass-transfer limitations, but especially by the deactivation of the catalytic functions due to the high sensitivity of Pd towards a broad range of groundwater constituents [15–18]. Naturally-occurring reduced sulphur species, such as dimethyl sulphide, diethyl sulphide, SO₃²⁻, HS⁻, S²⁻ and H₂S, can strongly bind to Pd, inducing structural and electronic effects which result in loss of activity or shift in selectivity—so-called catalyst

* Corresponding author. Fax: +49 341235451760.

E-mail address: katrin.mackenzie@ufz.de (K. Mackenzie).

poisoning [19,20]. Even though Davie et al. [14] came to the conclusion that Pd-based catalysis is already economically competitive with other detoxification methods (such as air stripping, permeable reactive barrier or active-carbon sorption), the problems associated with catalyst regeneration [13,16–18,21] strongly hinder its use in environmental practice. The currently accepted opinion is that further research efforts have to be made in the direction of catalyst protection rather than focusing on intrinsic activity improvements [22]. Promising protection approaches include the use of Pd-doped hydrophobic zeolites or polymeric membranes to shield the catalyst from poisons [23–26]. In theory, hydrophobic non-porous polymeric membranes are able to enrich the organic compounds in the vicinity of the catalyst centres by partitioning from the water phase. Thus, the catalytic surface is protected from ionic compounds, metal ions and macromolecules. Poly(dimethylsiloxane) (PDMS), a well-known and extensively used rubbery polymer [27], has been chosen by our group as protecting material due to its outstanding properties, such as chemical stability, non-toxicity, high hydrophobicity and easy handling. In particular, the flexibility of the O–Si–O backbone structure, its low glass transition temperature ($\approx -125^\circ\text{C}$) and its high diffusivity make PDMS extremely well permeable to non-ionic compounds [28,29]. In previous reports on our research, the batch catalytic properties of PDMS membranes containing Pd/Al₂O₃ [25,26] or Pd clusters [24] have been studied, showing promising results in performance and stability. However, although the batch system is useful for screening of the catalyst's basic properties, it cannot be reliably used to predict the behaviour in treatment plants, where the catalyst is presumably stressed by high and varying concentrations of CHC and poisons. Subject of the present work are the further development of the discontinuous batch system and the understanding of the properties of supported and unsupported Pd catalysts embedded in PDMS layers for continuously operated semi-batch mixed-flow-reactors (MFR). The catalytic Pd-PDMS material has been applied as coating on reactor walls or covering the surface of glass rings, which then can be used as packing material in fixed-bed reactors. Special attention has been given here to the long term performance of embedded Pd catalysts, their stability against internal and external poisons and to the influence of mass-transfer effects in different reactor configurations. The outcomes of this research represent a useful and necessary step towards the implementation of PDMS-protected Pd systems in water treatment facilities.

2. Materials and methods

2.1. Chemicals

Reagents, Pd salts and CHCs were purchased in the highest available grade from Merck, Sigma–Aldrich or Chempur (Germany) and used as received. SilGel® 612 A/B, a two-component PDMS precursor, was purchased from Wacker-Chemie, Germany. Activated carbon (PKD, grain size ca. 75 μm) was purchased from Carbotech, Germany. The eggshell catalyst G-133D with nominal 0.5 wt-% Pd on γ -Al₂O₃ was purchased from Commercia, Germany, crushed and sieved prior to use; the size fraction $d_p < 25 \mu\text{m}$ was used for the HDC experiments and analysed for its BET surface area (161 m^2/g , N₂ adsorption), porosity (0.43 cm^3/g , N₂ adsorption), Pd content and dispersion ($x_{\text{Pd}} = 0.51$ wt-% by XRF and $d_{\text{Pd}} = 0.16$ by CO chemisorption, respectively).

2.2. Polymer-coated catalysts

2.2.1. Wall-coated reactors

For Pd particles embedded in PDMS (PDMS-Pd), (i) 4.0 g of the PDMS blend (A and B components 2:1) were mixed into 15 mL hex-

ane and placed in a cylindrical glass vessel, which (ii) was allowed to rotate in horizontal position overnight (final treatment at 40 °C) in order to assure uniform distribution and curing of PDMS at the inner wall of the vessel. Then (iii) an aliquot of a solution of Pd(ac)₂ in THF (50 mg in 15 mL) was introduced into the vessel under continued rotation. After complete evaporation of the solvent, (iv) the incorporated Pd(II) was reduced to the catalytic active Pd(0) by flushing the system with N₂/H₂ for 30 min. The fast reduction is visible by colour change from yellow to black. For Pd/Al₂O₃ embedded in PDMS (Pd/Al₂O₃-PDMS) the procedure consists of steps (i) and (ii). In step (i), 50 mg of Pd/Al₂O₃ was added to the PDMS-hexane mixture. The average thickness of the resulting PDMS membranes was 200 μm for 250-mL vessels and 190 μm for 300-mL vessels.

2.2.2. Packed-bed reactors

Two different sizes of Raschig glass rings providing different surface area per bed volume were used as membrane carrier in a packed bed. The average mass per piece & geometric surface area were 270 mg and 12 cm^2/g for type A and 39 mg and 15 cm^2/g for type B, respectively (see Fig. S12 for details). In a typical coating procedure, the rings were dip-coated in a glass flask containing a homogeneous mixture of 2 volumes PDMS precursors and 1 volume hexane together with a given amount of suspended Pd/Al₂O₃ particles. The rings were then removed from the flask and dried at 70 °C. Rings of type A were coated with three different thicknesses of PDMS (7, 40 and 80 μm) having 7.3×10^{-5} , 4.9×10^{-4} and 4.8×10^{-4} wt-% of Pd, respectively. Rings of type B were coated with a PDMS layer of 33 μm having a Pd content of 8.4×10^{-4} wt-%. The batch tests and the long-term mixed-flow tests were performed in a reactor equipped with a perforated Teflon plate as spacer, thereby preventing the membranes on the rings from being damaged by the stirrer (see Fig. S11 for details).

2.3. Characterization of membranes

Physical and qualitative characterization of the membranes was performed by means of scanning electron microscopy (SEM, Zeiss, DSM982 Gemini) and energy-dispersive X-ray spectroscopy (EDX, NORAN Instruments, 984A-1SUS Pioneer Norvar SUN/Voyager).

2.4. Hydrodechlorination (HDC) experiments

The performance of the various types of Pd HDC catalysts (as particles, wall coated reactors and coated packed bed materials) was tested in closed batch systems (for screening of catalyst activities) and continuous mixed flow reactors (MFR) (preferably used for continuous longer-term experiments). Chlorobenzene (MCB), trichloroethene (TCE) and chloroform (CF) were chosen as model contaminants representing three classes of substrates: fast-reacting aromatic CHCs, fast-reacting aliphatic CHCs and slow-reacting CHCs, respectively [7]. The reaction kinetics was monitored by means of headspace analysis of educts and products using GC-MS (QP 2010, Shimadzu Corp., equipped with a 25 m DB1 capillary column) or GC-FID (GC 2010, Shimadzu Corp., equipped with 30 m HP5-MS and GS-Q capillary columns) devices. The chloride concentration in the reaction solution was regularly monitored via ion chromatography measurements (IC25, Dionex, IonPac AS11/AG15).

2.4.1. Batch reactivity screening

250-mL clear screw-cap bottles equipped with Mininert® valves were chosen as reaction vessels. After filling the vessels with 200 mL of slightly buffered reaction solution (NaHCO₃ 9 g/L) and purging with gaseous hydrogen for 15 min (pH = 8.7), the HDC was started by adding a methanolic CHC stock solution. The system was kept under continuous shaking (210 rpm on a horizontal shaker)

throughout the reaction, thus ensuring sufficient H_2 supply from the headspace reservoir to the reaction solution. In the case of the coated rings, the tests were performed in 300 mL-reactors equipped with a bearing plate and magnetic stirrer. Evaluation of the catalyst performance in batch screening tests was carried out defining the reaction kinetics per unit of volume of liquid and using the specific catalyst activity $A_{Pd,i}$ (for derivation see SI section) for the HDC of the CHC i according to Eq. (1) [7,8]:

$$A_{Pd} = \frac{1}{c_{Pd} \times \tau_{1/2}} = \frac{\ln(c_{t1}/c_{t2})}{\ln 2 \times c_{Pd} \times (t_2 - t_1)} \text{ in } [\text{L g}^{-1} \text{min}^{-1}] \quad (1)$$

where c_{Pd} is the Pd concentration related to the water volume, $\tau_{1/2}$ is the CHC's half-life (obtained from its disappearance kinetics), t_1 and t_2 are two arbitrarily chosen sampling times, and c_{t1} and c_{t2} are the corresponding CHC concentrations. The second part of Eq. (1) holds strictly only for a first-order kinetics with respect to the catalyst and reactant concentrations. The specific catalyst activities $A_{Pd,i}$ were calculated either from the CHC conversion data or from those of product formation. The value of $A_{Pd,i}$ is equivalent to a second-order rate coefficient as it is usually derived from an observed first-order rate coefficient k_{obs} [s^{-1}] according to $A_{Pd,i} = k_{obs}/(\ln 2 \cdot c_{Pd})$.

2.4.2. Reactivity in semi-batch mixed-flow reactors

A PDMS-coated vessel (or a packed-bed reactor) was filled with 200 mL of slightly buffered solution (NaHCO_3 9 g/L, $\text{pH} = 8.7$) and purged with H_2 for at least 15 min. While the vessel was kept under constant shaking or stirring, the HDC was started by connecting the reaction vessel to a hydrogen flow (15 mL/min). The gas flow was continuously loaded with the target compound (CHCs or cyclohexene) by flushing through an activated-carbon (AC) reservoir (Fig. S11), which contained 300 g of activated carbon suspended in 700 mL of deionized water. The reservoir was regularly spiked with methanolic stock solutions of the target compounds. Steady desorption and stripping of the AC-bound CHC into the H_2 flow assured a long-lasting CHC supply to the reactor with only slow concentration decline. The CHC initial incoming concentration used was in the range of 5–80 $\mu\text{mol/L}$. Mixing was assured for wall-coated reactors by an external shaker and for packed-bed reactors by an internal stirrer. Reaction kinetics was monitored by sampling the incoming and outgoing gas flows and the water phase. For each sampling point, the specific activity $A_{Pd,i}$ was calculated by adapting the performance equation of steady-state mixed-flow reactors for first-order reaction kinetics Eq. (2) [30]:

$$A_{Pd} = \frac{F_{in} \times K_H \times (c_{in,CHC}/c_{out,CHC})^{-1}}{0.69 \times c_{Pd} \times V_W} \\ = \frac{F_{in} \times K_H \times (c_{out,alkane}/c_{out,CHC})}{0.69 \times c_{Pd} \times V_W} \text{ in } [\text{L g}^{-1} \text{min}^{-1}] \quad (2)$$

where F_{in} is the incoming flow of hydrogen, K_H is the dimensionless Henry's law constant of the reactant. CHC and $alkane$ are the reactant and its product, c_{in} and c_{out} are the molar concentrations in the gas flow before and after the reactor, c_{Pd} is the Pd concentration in g/L and V_W is the volume of the water phase. A summary on the kinetic evaluation of first-order HDC reactions in batch systems in presence of the sorption-active PDMS material is given in the SI section.

Eq. (2) yields an approximation of the real catalyst activity, since it is based on a first-order kinetics with respect to the dissolved fraction of CHC. As will be discussed later in this study, there can also be significant contributions of the gaseous and the PDMS-sorbed CHC fractions to the overall conversion. A_{Pd} as defined in Eq. (2) does not include such contributions and therefore reflects an apparent catalyst activity. Nevertheless, A_{Pd} provides a tool for comparing the performance of various catalytic systems in long-term studies

carried out under constant experimental conditions. In the following experiments, A_{Pd} is plotted against reactor operation time or TON (turnover number). TON has been derived by calculating the amount of CHC converted for each sampling point i according to Eqs. (3) and (4):

$$\text{TON} = \frac{n_{\text{CHC,converted}} \text{ in mol}_{\text{CHC}} \text{ mol}_{\text{Pd}}^{-1}}{n_{\text{Pd}}} \quad (3)$$

$$n_{\text{CHC,converted}} = \sum_i \left(F_{i,in} \times (t_i - t_{i-1}) \times \left(\frac{(1 - c_{t_i,CHCout})}{c_{t_i,CHCin}} \right) \times c_{\text{CHC,in}} \right) \quad (4)$$

where $F_{i,in}$ is the incoming gas flow, t_i is the sampling time and $c_{t_i,CHCout}$ and $c_{t_i,CHCin}$ are the molar concentrations of the reactant in the gas flow before and after the reactor. Unlike the operation time, the TON allows an immediate comparison of the catalysts stability based on the converted amount of reactant.

2.5. Catalyst poisoning by sulphur compounds, HDC self-poisoning and mass-transfer effects

The protection of the PDMS coating against naturally occurring ionic poisons was tested by adding Na_2SO_3 as a model compound for reduced ionic sulphur species. The self-poisoning effect by chloride produced from HDC was contrasted with a non-chloride-producing reaction: the hydrogenation of cyclohexene combined with a subsequent spiking of the reaction medium with CHC. The determination of retained chloride was performed indirectly by measuring the chloride released to the water phase. In order to verify the presence of mass-transfer limitation at the water/PDMS boundary layer, a long-term HDC test was performed in a mixed-flow reactor using TCE and chloroform as target compounds, differing by 4 orders of magnitude in their intrinsic HDC reactivities [7].

3. Results and discussion

3.1. HDC performance

3.1.1. HDC batch experiments

Fig. 1 shows typical kinetic profiles found in batch MCB hydrodechlorination experiments with catalytic PDMS membranes coating the wall of the batch reactor. The addition of a polymeric barrier between the contaminated water and the catalytic sites naturally affects the reaction rate. On the one hand, the membrane is an additional hindrance, limiting mass-transfer rates. On the other hand, sorption enriches the CHCs in the hydrophobic PDMS matrix close to the catalytic centres. Sorption is faster than the chemical reaction under the applied conditions, such that the partitioning is close to equilibrium (initial absorption of about 79% of $C_{0,\text{MCB}}$, within 2 min). Hence, the linearity and the slopes of the kinetic curves are not affected.

The only effects are an ordinate intercept different from zero and an offset between the educt- and product-stemmed pseudo-first order plots (Fig. 1a).

Mass-transfer limitations are a sum of effects including (i) diffusion of reactants in the stagnant water boundary layer (film effect at the water/PDMS interface), (ii) diffusion within the PDMS layer (matrix diffusion), and (iii) diffusion inside the porous catalyst carrier (in the case of embedded supported catalyst $\text{Pd}/\text{Al}_2\text{O}_3$). Reported specific activities for MCB conversion with water-suspended $\text{Pd}/\text{Al}_2\text{O}_3$ or Pd colloids are in the order of $200\text{--}300 \text{ L g}^{-1} \text{ min}^{-1}$ or $400 \text{ L g}^{-1} \text{ min}^{-1}$, respectively [7,8]. For PDMS-embedded catalysts, a decrease of A_{Pd} by one order of magnitude has been found for $\text{Pd}/\text{Al}_2\text{O}_3$ (see Fig. 1b and [25]), while for the embedded Pd NPs the drop reaches two orders of magnitude, decreasing from 400 to $2 \text{ L g}^{-1} \text{ min}^{-1}$ (Fig. 1a). In order to discuss

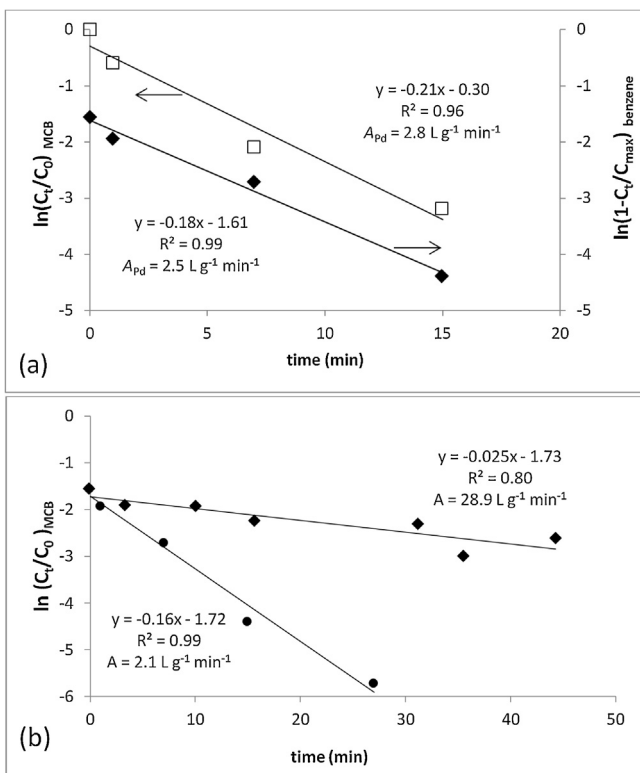


Fig. 1. Kinetic curves representing first-order kinetics of MCB hydrodechlorination in a wall-coated batch reactor system. (a) Comparison of kinetic profiles from MCB depletion (open symbols) and benzene formation (filled symbols) in a PDMS-coated reactor with Pd NPs, $C_0, \text{MCB} = 13.8 \text{ mg/L}$, $C_{\text{Pd}} = 103.5 \text{ mg/L}$. (b) Kinetic profile of MCB depletion in a PDMS-coated reactor with embedded Pd/Al₂O₃ (0.5% wt-% Pd, squared symbols) and with Pd clusters generated within the membrane (circles), $C_0, \text{MCB} = 13.8 \text{ mg/L}$, $C_{\text{Pd-cluster}} = 105 \text{ mg/L}$, $C_{\text{Pd as Pd/Al}_2\text{O}_3} = 1.26 \text{ mg/L}$, $m_{\text{PDMS}} = 4.1 \text{ g}$, $d_{\text{membrane}} = 190 \mu\text{m}$.

this differences it is helpful to remember the modified preparation procedures of the active membranes: while the incorporation of supported Pd is carried out with a 'one-pot' system where the dispersion of the Pd clusters on the alumina surface remains largely unaffected, the procedure for unsupported Pd species involves diffusion and reduction steps which might affect the size and spatial distribution of Pd species in the PDMS matrix. Therefore, one reason for the unexpectedly low Pd activity in PDMS-Pd might be the uneven size distribution of Pd particles, where the larger particles may comprise a significant mass fraction of Pd but exhibit a small surface fraction only (compare SEM analysis, Fig. SI3).

The different activity losses for the two catalysts employed could be caused not only by the distribution of Pd but also by the influence of catalyst surroundings. Additional HDC experiments with Pd/Al₂O₃ suspended in various solvents and solvent mixtures (hexane, THF and THF-water mixtures) showed that the reaction rates increase with increasing water content in the reaction medium ([25] and own data, not shown here). However, even in a dry solvent such as n-hexane significant HDC rates were measured ($A_{\text{Pd}} = 18 \dots 28 \text{ L g}^{-1} \text{ min}^{-1}$ [25]). This means that although water is a promoting solvent for HDC reaction, it is not essential for HCl desorption. Unlike the unsupported Pd in Pd-PDMS, whose surface is in direct contact with the organic polymer phase, the Pd in the pores of γ -alumina is assumed to be surrounded by (highly acidic) pore water. The aqueous micro-environment could lead to a faster HDC reaction.

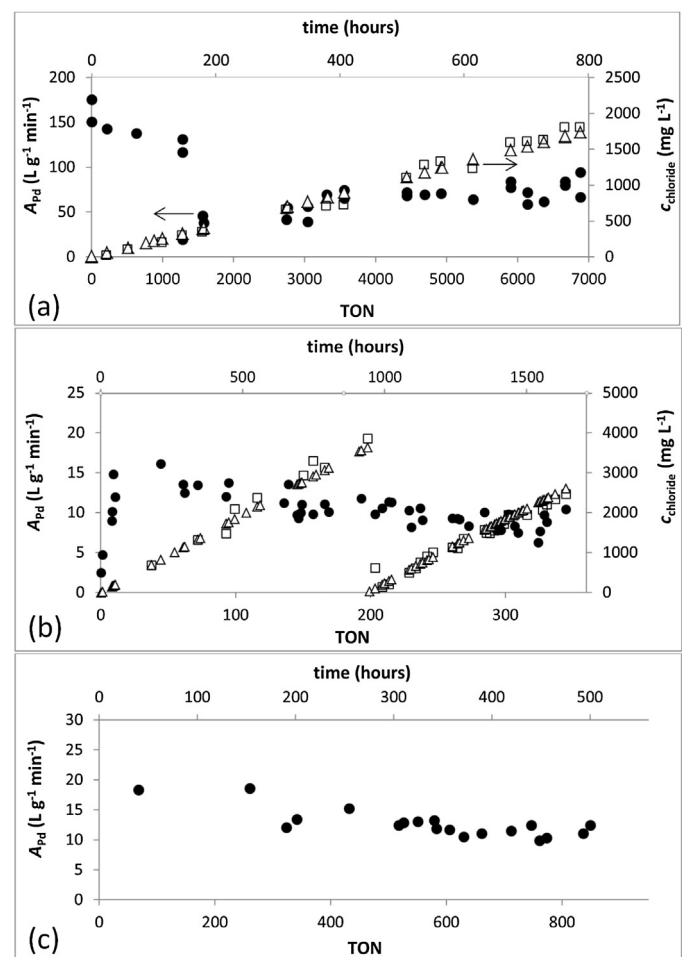


Fig. 2. Trend of the specific Pd activity (●) in various long-term HDC experiments with TCE in continuously fed mixed-flow reactors using: (a) A PDMS-Pd/Al₂O₃ wall-coated reactor, medium water filling level ($m_{\text{catalyst}} = 58.8 \text{ mg}$, $m_{\text{PDMS}} = 4.1 \text{ g}$, $d_{\text{membrane}} = 190 \mu\text{m}$); (b) A PDMS-Pd-wall-coated reactor ($m_{\text{pd}} = 21.8 \text{ mg}$, $m_{\text{PDMS}} = 4.1 \text{ g}$, $d_{\text{membrane}} = 190 \mu\text{m}$; at TON = 200 the reactor was emptied and re-filled with fresh reaction solution); (c) A packed bed with 52.4 g of PDMS-Pd/Al₂O₃-coated glass rings type B ($m_{\text{catalyst}} = 87.9 \text{ mg}$, $m_{\text{PDMS}} = 2.4 \text{ g}$, $d_{\text{membrane}} = 33 \mu\text{m}$). For (a) and (b) calculated (Δ) and measured (□) chloride concentrations in the aqueous bulk phase are given.

3.1.2. Long-term HDC performance

The regime of real flow-through reactors is expected to be between two ideal reactor limits: the ideal mixed-flow reactor (MFR) and the ideal plug-flow reactor [30]. Because of the lower concentration gradients within a MFR, we chose this reactor type in a semi-batch set-up for long-term hydrodechlorination experiments: it allows a better control of the reaction conditions in the three-phase reactor including the carrier gas flow ($\text{H}_2 + \text{reactants}$), a stirred water phase and the PDMS wall coating containing the catalyst. For the same MFR set-up, two different configurations, wall-coated reactor and packed bed, were used (Fig. SI1). The packed bed system has two main advantages: (i) possibility of tuning the amount of catalyst in the reactor, (ii) avoiding the overlap of water- and gas-phase reaction rates (Section 3.3).

Catalyst activity and stability

Fig. 2 shows the activity trend in three long-term HDC experiments with Pd/PDMS-systems plotted against the turnover number (TON). The catalysts used are (a) PDMS-embedded Pd/Al₂O₃ as wall-coating membrane, (b) a wall-coating membrane containing *in-situ* generated Pd clusters and (c) PDMS-embedded Pd/Al₂O₃ as membrane covering glass rings which are arranged as fixed bed. In addition to the activity trend, measured and the theoretically cal-

culated chloride concentrations are also shown for the wall-coated reactor experiments. The initial Pd activity of the wall-embedded supported catalyst is about half that of the freely suspended catalyst: $A_{\text{Pd}} \approx 170 \text{ L g}^{-1} \text{ min}^{-1}$ vs. $\approx 300 \text{ L g}^{-1} \text{ min}^{-1}$. This is much higher than expected from previous experiments. A closer inspection of the reactor design revealed that the geometry and phase conditions of the reactor play a major role here: the upper part of the PDMS membrane was in contact with the headspace phase and, therefore, less affected by the film effect at the water/PDMS interface (see Section 3.3). In contrast to the reactor design used in long-term experiments with wall coating, in the packed-bed reactor the PDMS/catalyst layer was placed entirely inside the aqueous phase. This design led to a 10-fold decrease in initial Pd activity, compared to the freely suspended catalyst particles (Fig. SI5 and SI6).

Independent of the reactor type, the specific activity decreased over time in all cases. This phenomenon has been observed for Pd catalysts under different reaction conditions and has been attributed to various causes, such as chloride formation during HDC [31]. The deactivation trend is less pronounced when using the continuous HDC set-up than when using discontinuously repeated batch experiments for long-term operation (Fig. SI5 and SI6). After ten HDC batch cycles conducted with a Pd/Al₂O₃-PDMS wall-coated vessel (TON = 750), less than 50% of the initial Pd activity remained ([25] and this study), whereas the catalyst in the continuously operated long-term system established a relatively stable activity level allowing a much longer catalyst life time (Fig. 2a). Naturally, the embedding itself leads to an activity loss compared to the uncoated particles (compare A_{Pd} in Fig. SI6 and 2a). This effect is more pronounced for the unsupported Pd, where the metal surface is in direct contact with the PDMS (compare $A_{\text{Pd}} \approx 500\text{--}1000 \text{ L g}^{-1} \text{ min}^{-1}$ for Pd colloids to $A_{\text{Pd}} \approx 10\text{--}15 \text{ L g}^{-1} \text{ min}^{-1}$ in Fig. 2b), than for supported porous catalysts such as Pd/Al₂O₃. In order to understand these findings we have to look at the major causes of Pd catalyst deactivation in the absence of 'external' poisons. Sintering of Pd crystallites, HCl attack, formation of carbonaceous deposits and Pd leaching due to local pH decrease are believed to contribute to Pd deactivation [15,32]. The Pd catalyst in the described long-term set-ups seems to benefit from the persistence of semi-batch conditions and a sufficient hydrogen supply, which may contribute to a continuous regeneration of the Pd surface from weakly deactivating species or prevent their formation. Indeed, hydrogen suppresses the formation of radical-born oligomers on the Pd surface [32] and is commonly used for regenerating Pd surfaces [33]. Fig. 2(a–c) shows that the Pd catalysts undergo a short 'conditioning phase' where their activity rises. This may also be attributed to the action of hydrogen (probably reducing some surface-bound Pd oxide). In the case of the polymer-embedded catalysts, HDC by-products such as HCl can contribute to catalyst deactivation when they cannot be released from the polymer matrix. It is reasonable to assume that chloride formed in HDC can leave the polymer as molecular HCl and diffuse into the water bulk phase. In the case of micro-habitats filled with liquid water (e.g. in the γ -alumina pores) a highly concentrated hydrochloric acid may be accumulated. A proportion of the HCl may not reach the bulk water phase and could instead (i) react with the Pd surface or (ii) promote the hydrolytic degradation of PDMS. Based upon this premise, it may be expected that the two catalyst types – embedded bare Pd particles and supported Pd clusters – experience different HCl deactivation. The impact of HCl upon the Pd surface is common to both types.

The unsupported Pd should be more affected by the PDMS degradation, whereas the Pd fixed in the alumina pores should be more affected by local highly acidic conditions in water-filled pores. The results shown in Fig. 2 suggest that the effect of polymer degradation on Pd activity is most significant, making Pd/Al₂O₃ more

long-term resistant. Moreover, alumina can act to a certain extent as HCl scavenger and moderate acidic Pd leaching. As reported, alumina can relieve the Pd surface from Cl adsorption better than organic carriers [34]. The sum of these effects could explain the faster deactivation observed for the embedded unsupported Pd particles (compare Figs. 2a and c with Fig. 2b up to TON = 300). Even though the experiments displayed in Fig. 2a and b shows a complete release of chloride (up to a TON of 7000 and 350, respectively), traces of HCl which might remain in the membrane would not be detectable from the chlorine balance (amount of chloride in the bulk water phase/amount of degraded CHC). Furthermore, in several experiments the chloride release was incomplete. Previous batch experiments performed with Pd/Al₂O₃-PDMS showed gaps up to 50% in the chlorine balance at TON ≤ 750 [25], suggesting that a better chloride release takes place in continuously operated long-time experiments. This might be the reason for the higher long-term stability found for Pd/Al₂O₃-PDMS in HDC experiments.

In order to distinguish between chlorine-caused effects and other deactivation mechanisms, we used the hydrogenation of cyclohexene as a probe reaction for the long-term behaviour of a PDMS-Pd/Al₂O₃-coated reactor. During the continuously running hydrogenation, TCE was spiked regularly and the effect of short HDC periods on the hydrogenation activity was monitored. The conversion of TCE was confirmed by measuring the ethane produced. Each TCE spike corresponded to 45 μmol of HCl produced, yielding a ratio of $n_{\text{Cl}}:n_{\text{Pd}} = 18 \text{ mol/mol}$. As it is obvious from Fig. 3, the HDC of TCE strongly affects the hydrogenation of cyclohexene and causes a sudden drop in hydrogenation rates immediately after TCE addition. Once the TCE is fully removed after less than 1 h, the hydrogenation activity slowly rises again up to pre-addition values. After about one week on-stream, the catalyst activity declined without any acute TCE impact. Under these conditions at the lower activity level, additional TCE spikes did not further deactivate the catalyst. We draw two conclusions from Fig. 3: (i) the HDC of TCE strongly affects the hydrogenation activity of Pd/Al₂O₃-PDMS whereby the Pd deactivation is probably not due to TCE itself (which is rapidly removed from the aqueous and gas phase) but due to the *in-situ* produced HCl, and (ii) this deactivation is reversible under the reaction conditions. The formed HCl did not significantly affect the pH value of the bulk water phase, which was buffered at about 8.7 by NaHCO₃.

An abrupt activity decrease similar to that shown in Fig. 3 was also observed for the long-term HDC with the same type of catalyst (Fig. 2a, TON > 1100).

This suggests that the deactivation behaviour of embedded Pd/Al₂O₃ is different from that of Pd clusters, where the Pd activity does not show any sudden decline (Fig. 2b). Further studies are necessary in order to explain this behaviour. A very high initial apparent Pd activity of $A_{\text{Pd}} = 1600 \text{ L g}^{-1} \text{ min}^{-1}$ for the hydrogenation reaction is remarkable, which emphasizes the great potential of the membrane-based catalyst in the absence of adverse effects. However, this value cannot be directly compared with TCE hydrodechlorination in batch experiments, since the activity formula does not include the residence time of substrates enriched in the PDMS phase.

3.2. Catalyst stress tests with added poisons

Sulphite was chosen as probe to investigate the resistance of Pd catalysts against ionic catalyst poisons. The catalyst activities were compared before and after sulphite addition in a running batch experiment. According to the pK_a -values of sulphurous acid (1.8 and 7), SO₃²⁻ is the predominant species under alkaline conditions (in our case, pH = 8.7). Usually we used atomic ratios of S: Pd_{total} ≥ 3 in order to provoke the complete fouling of the unprotected Pd function. We studied the poisoning effect of sodium sulphite in

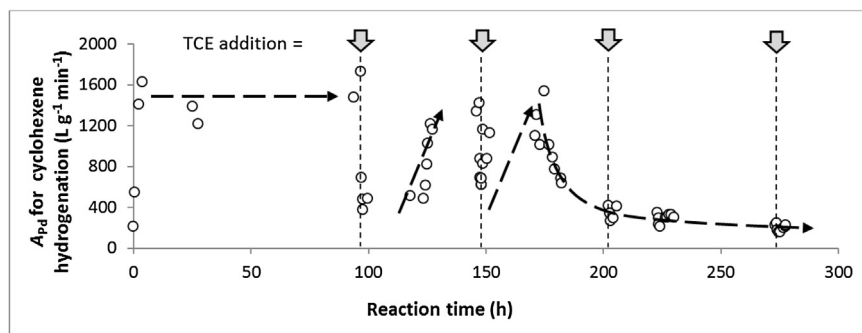


Fig. 3. Long-term hydrogenation of cyclohexene performed using a PDMS-Pd/Al₂O₃ wall-coated reactor ($m_{\text{Pd/Al}_2\text{O}_3} = 51.2 \text{ mg}$, $m_{\text{PDMS}} = 4.05 \text{ g}$, $d_{\text{membrane}} = 190 \mu\text{m}$). Dashed arrows represent the trend of hydrogenation activity.

standard batch tests for Pd/Al₂O₃-PDMS and in long-term experiments for Pd-PDMS.

3.2.1. Pd/Al₂O₃-PDMS

In a previous study we have shown that the stability of embedded Pd against sulphite for PDMS-Pd/Al₂O₃ wall-coated reactors in batch HDC increased with the membrane thickness [25]. Catalysts embedded within 150 μm thick membranes remained totally protected against 1 mM sulphite (S: Pd of 400), while with 10 mM sulphite some deactivation was observed. Unprotected Pd catalysts are rapidly and completely deactivated in the presence of 1 mM sulphite (data not shown). In this work, the effect of sulphite addition on thinner membranes containing Pd/Al₂O₃ was examined by means of standard batch stress tests with high S: Pd ratios. Fig. 4a shows the kinetic profile of two batch HDC experiments using TCE as probe molecule, carried out with glass coated rings carrying a 7 μm thick Pd/Al₂O₃-PDMS membrane. The effect of sulphite poisoning is expressed as the ratio between the rate constants before and after sulphite addition (k and k_p , respectively). Similar tests with thicker PDMS coatings (40 μm and 80 μm) were also performed, showing no immediate poisoning effect. At low membrane thicknesses, sulphite does not fully deactivate the catalyst, whose activity is reduced to about 50% by 1 mM sulphite (S: Pd = 1200) and to 20% by 11 mM sulphite. This reduction can possibly be attributed to uncovered Pd/Al₂O₃ close to the surface which naturally receives less protection by a thin membrane.

3.2.2. Pd-PDMS

For the unsupported catalyst, the protection offered by the PDMS is expected to be the same as reported for Pd supported on alumina. Nevertheless, experimental evidence suggests that the majority of the catalyst is located closer to the membrane surface (see Section 3.1) and therefore more susceptible to poisoning attack. In order to verify the resistance of Pd-PDMS membranes, increasing concentrations of sulphite were added into a Pd-PDMS-coated reactor (membrane thickness 190 μm). The effects of two consecutive additions of Na₂SO₃ (1 mM) to the reaction system are displayed in Fig. 4b. The activity is completely maintained after the first addition but clearly decreases after the second one. This means that even after the addition of sulphite with a ratio as low as S: Pd = 2, the catalyst is partially deactivated. Under the assumption that the membrane quality for incorporated Pd/Al₂O₃ and Pd clusters is identical, this indicates that a considerable proportion of the Pd lacking protection is located near the membrane surface. For enhanced protection, a more favourable distribution of palladium in the PDMS film, i.e. less Pd near the surface, should be achieved either by tuning the preparation conditions (swelling solvent and type of Pd precursor, temperature of Pd reduction, type of reductant) or by applying a second layer of PDMS. Optimization of the Pd-membrane synthesis will be subject of a forthcoming paper.

3.3. Mass-transfer effects for PDMS-embedded Pd catalysts

As shown earlier, catalyst protection via PDMS membranes is associated with significant loss of catalytic activity. Although an undesired phenomenon, it is probably inevitable. For optimization of the catalyst design the present studies were focused on minimizing mass-transfer effects and catalyst deactivation.

Considering the path of the CHC molecule, it has to be transferred (i) from the bulk water phase to the polymer surface, (ii) through the bulk polymer to the surface of Pd or alumina particles and, in the case of supported palladium, (iii) from the external alumina particle surface through its pore network to the Pd sites. All these processes are diffusion-controlled. For mass-transfer-limited reactions, one or several of these steps may affect the overall rate of the reaction, lowering the catalyst's apparent activity, especially for fast-reacting compounds (such as TCE and MCB). Under the applied reaction conditions, it is reasonable to assume that the diffusive transfer of reactants through a stagnant boundary layer (SBL) in the water phase is the major limitation. This hypothesis was checked by means of a competition experiment shown in Fig. 5. A long-term HDC was carried out using TCE as fast-reacting compound and chloroform (CF) as slowly-reacting compound. The rate constant of TCE conversion is a factor of 500 higher than that of CF (with Pd/Al₂O₃ 63–125 μm , $A_{\text{Pd}} = 420$ and $0.8 \text{ L g}^{-1} \text{ m}^{-1}$, respectively [7]). It must be expected that the conversion rate of the fast-reacting compound is more affected by changes in the mass-transfer conditions than that of the slowly-reacting compound. During the running experiment, the volume of the water phase (WP), and therefore the ratio between gas-exposed and water-exposed PDMS surface areas, was stepwise changed. As is obvious from Fig. 5, the TCE conversion rate increased with increasing headspace volume, while that of CF remained fairly constant. This has also been demonstrated in corresponding batch experiments (data not shown here). However, as stated above, Eq. (2) only applies for the reaction in the water phase. Therefore, only semi-quantitative conclusions are allowed from the apparent catalyst activities A_{Pd} . Qualitatively, the experimental results obtained confirm the hypothesis of external mass-transfer limitations. It is reasonable to assume that a thin water film is always present on the PDMS membrane, even for that part which is exposed to the (water saturated) gas phase. The thicknesses of the two stagnant water layers may ultimately control the external mass-transfer rates from the two compartments of the reactor: water phase and headspace phase. However, both film thicknesses are not directly measurable. The diffusion coefficients ($D_{\text{CHC}} \text{ in water} \approx 10^{-9} \text{ m}^2 \text{ s}^{-1}$) are equal, whereas the ratio of the two CHC concentrations are given by the dimensionless Henry's law coefficients $K_{\text{H,i}}^{20^\circ\text{C}} = c_{\text{i,gas}}/c_{\text{i,water}} = 0.43$ for TCE and 0.13 for CF.

In order to overcome mass-transfer limitations and to exploit the high intrinsic catalytic activity of Pd more effectively, the SBL can be reduced by increasing the agitation intensity. Alternatively,

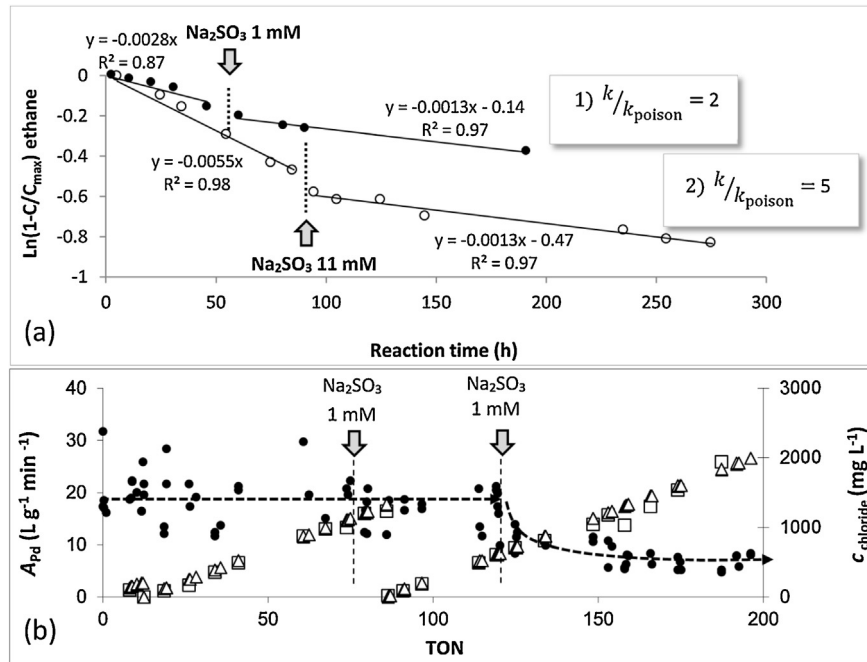


Fig. 4. (a) Influence of Na_2SO_3 addition during TCE HDC batch tests with PDMS-Pd/ Al_2O_3 coated rings type A ($c_{\text{Pd}} = 0.09 \text{ mg/L}$, $d_{\text{membrane}} = 7 \mu\text{m}$, dashed line marks addition of Na_2SO_3 , S: Pd ratios: 1) 1,200, 2) 12,800. (b) Long-term HDC of TCE with PDMS-Pd and twice adding catalyst poison ($c_{\text{Pd}} = 21 \text{ mg/L}$, $d_{\text{membrane}} = 190 \mu\text{m}$, arrows marks addition of Na_2SO_3 , S: Pd = 1). Concentration of released chloride is displayed on the secondary ordinate. After t corresponding to TON = 86, the reactor was emptied and re-filled with fresh reaction solution. Dashed trend lines for Pd activity are added to guide the eye.

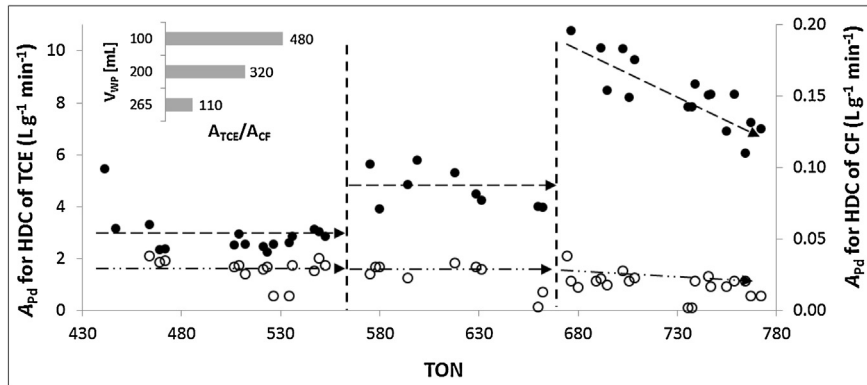


Fig. 5. Influence of variation of water phase volume and therefore membrane coverage by water in a semi-batch mixed-flow reactor on the apparent Pd activity of PDMS-Pd ($m_{\text{Pd}} = 21.8 \text{ mg}$, $m_{\text{PDMS}} = 4.1 \text{ g}$, $d_{\text{membrane}} = 190 \mu\text{m}$). Up to TON = 560 $V_{\text{water}} = 265 \text{ mL}$ (PDMS-Pd entirely covered), for TON = 560–670 $V_{\text{water}} = 200 \text{ mL}$, from TON = 670 $V_{\text{water}} = 100 \text{ mL}$. Filled symbols: A_{Pd} for HDC of TCE, empty symbols: A_{Pd} for HDC of CF.

the reactor can be redesigned taking into consideration the lower mass-transfer resistance from the gas phase. This idea was realized in a trickle-bed reactor (TBR), where the contaminated water was trickled over a catalytic fixed-bed under a concurrent or counter-current hydrogen flow. Studies of the TBR may also show whether or not there is a positive effect of a thin SBL and may provide further useful knowledge about another kind of potentially applicable reactor design.

4. Conclusions

The study of the catalytic behaviour of PDMS-embedded Pd/ Al_2O_3 microparticles and Pd nanoparticles represents a step towards the implementation of the Pd-PDMS technology for detoxification of chlorohydrocarbon-contaminated waters. PDMS can efficiently protect the Pd from common ionic poisons and macromolecules, without compromising the conversion rates. The loss of Pd activity due to embedding into the PDMS membrane is

inevitable. Highly active catalyst particles (e.g. Pd colloids) show a much more pronounced relative loss of their initial catalytic activity compared to their less reactive pendants (e.g. Pd/ Al_2O_3). Employment of techniques for high particle dispersion in the membrane and higher membrane loading could reduce the activity loss and lead to higher performance. Nevertheless, for practical use, long-term stability of the catalysts is more valuable.

The work has paid particular attention to the phenomenon of Pd-PDMS deactivation: HDC self-poisoning or external sulphur poisoning. Results showed that embedded Pd utilized in continuously operated semi-batch mixed-flow reactors has a higher and longer-lasting stability against natural and self-deactivation than when used batch-wise in discontinuously operated reactors. The degradation of the polymer due to HCl attack appears to be responsible for the faster deactivation of the unsupported (bare Pd) catalyst. Studies of mass-transfer limitations of the membrane system led to recommendations for technical implementation: the performance of Pd-PDMS systems would benefit from the use of a reactor

design allowing the membrane to come into contact with both CHC-carrying phases (e.g. a trickle-bed reactor).

Acknowledgement

The study was conducted in the framework of the “NanoPOP” project, funded by the German Ministry of Education and Research (BMBF, FKZ 03×3571B). Special thanks go to Matthias Werheid (Department of Physical Chemistry, Dresden University of Technology) for conducting the SEM analyses and for fruitful discussions.

Appendix A. Supplementary data

Supplementary data associated with this article can be found, in the online version, at <http://dx.doi.org/10.1016/j.apcatb.2015.12.043>.

References

- [1] C.G. Schreier, M. Reinhard, *Chemosphere* 31 (1995) 3475–3487.
- [2] Y.I. Matatov-Meytal, M. Sheintuch, *Ind. Eng. Chem. Res.* 37 (1998) 309–326.
- [3] G.V. Lowry, M. Reinhard, *Environ. Sci. Technol.* 33 (1999) 1905–1910.
- [4] F.-D. Kopinke, K. Mackenzie, R. Koehler, *Appl. Catal. B* 44 (2003) 15–24.
- [5] B.P. Chaplin, M. Reinhard, W.F. Schneider, C. Schueth, J.R. Shapley, T.J. Strathmann, C.J. Werth, *Environ. Sci. Technol.* 46 (2012) 3655–3670.
- [6] M.A. Keane, *ChemCatChem* 3 (2011) 800–821.
- [7] K. Mackenzie, H. Frenzel, F.-D. Kopinke, *Appl. Catal. B* 63 (2006) 161–167.
- [8] H. Hildebrand, K. Mackenzie, F.-D. Kopinke, *Environ. Sci. Technol.* 43 (2009) 3254–3259.
- [9] Z. Zhao, Y.-L. Fang, P.J.J. Alvarez, M.S. Wong, *Appl. Catal. B* 140–141 (2013) 468–477.
- [10] H.-L. Lien, W.-X. Zhang, *Appl. Catal. B* 77 (2007) 110–116.
- [11] N.E. Korte, J.L. Zutman, R.M. Schlosser, L. Liang, B. Gu, Q. Fernando, *Waste Manag.* 20 (2000) 687–694.
- [12] W.W. McNab Jr., R. Ruiz, *Environ. Sci. Technol.* 34 (2000) 149–153.
- [13] C. Schueth, N.-A. Kummer, C. Weidenthaler, H. Schad, *Appl. Catal. B* 52 (2004) 197–203.
- [14] M.G. Davie, H. Cheng, G. Hopkins, C. Lebron, M. Reinhard, *Environ. Sci. Technol.* 42 (2008) 8908–8915.
- [15] P. Albers, J. Pietsch, S.F. Parker, *J. Mol. Catal. A* 173 (2001) 275–286.
- [16] G.V. Lowry, M. Reinhard, *Environ. Sci. Technol.* 34 (2000) 3217–3223.
- [17] D. Angeles-Wedler, K. Mackenzie, F.-D. Kopinke, *Environ. Sci. Technol.* 42 (2008) 5734–5739.
- [18] B.P. Chaplin, J.R. Shapley, C.J. Werth, *Environ. Sci. Technol.* 41 (2007) 5491–5497.
- [19] P.A. Gravil, H. Toulhoat, *Surf. Sci.* 430 (2009) 176–191.
- [20] N.S. Figoli, P.C. L'Argentiere, *J. Mol. Catal. A* 122 (1997) 141–146.
- [21] D. Angeles-Wedler, K. Mackenzie, F.-D. Kopinke, *Appl. Catal. B* 90 (2009) 613–617.
- [22] F.-D. Kopinke, *Environ. Sci. Technol.* 46 (2012) 11467–11468.
- [23] C. Schueth, S. Disser, F. Schueth, M. Reinhard, *Appl. Catal. B* 28 (2000) 147–152.
- [24] D. Fritsch, K. Kuhr, K. Mackenzie, F.-D. Kopinke, *Catal. Today* 82 (2003) 105–118.
- [25] R. Navon, S. Eldad, K. Mackenzie, F.-D. Kopinke, *Appl. Catal. B* 119–120 (2012) 241–247.
- [26] F.-D. Kopinke, D. Angeles-Wedler, D. Fritsch, K. Mackenzie, *Appl. Catal. B* 96 (2010) 323–328.
- [27] S. Seethapathy, T. Górecki, *Anal. Chim. Acta* 750 (2012) 48–62.
- [28] T.C. Merkel, R.P. Gupta, B.S. Turk, B.D. Freeman, *J. Membrane Sci.* 191 (2001) 85–94.
- [29] S.V. Dixon-Garrett, K. Nagai, B.D. Freeman, *J. Polym. Sci. Pol. Phys.* 38 (2000) 1461–1473.
- [30] O. Levenspiel, Chemical reaction engineering, in: *Ideal Reactors for a Single Reaction*, 3rd ed., John Wiley & Sons, New York, 1972 (Chapter 5).
- [31] S. Ordóñez, H. Sastre, F.V. Diez, *Appl. Catal. B* 40 (2003) 119–130.
- [32] J.W. Bae, E.D. Park, J.S. Lee, K.H. Lee, Y.G. Kim, S.H. Yeon, B.H. Sung, *Appl. Catal. A* 217 (2001) 79–89.
- [33] J.M. Jones, V.A. Dupont, R. Brydson, D.J. Fullerton, N.S. Nasri, A.B. Ross, A.V.K. Westwood, *Catal. Today* 81 (2003) 589–601.
- [34] G. Yuan, M.A. Keane, *Catal. Today* 88 (2003) 27–36.